ISPRS Journal of Photogrammetry and Remote Sensing 89 (2014) 59–66

Contents lists available at ScienceDirect

ISPRS Journal of Photogrammetry and Remote Sensing

journal homepage: www.elsevier.com/locate/isprsjprs

Effects of green space spatial pattern on land surface temperature: Implications for sustainable urban planning and climate change adaptation

Matthew Maimaitiyiming [a], Abduwasit Ghulam [a,*], Tashpolat Tiyip [b,c], Filiberto Pla [d], Pedro Latorre-Carmona [d], Ümüt Halik [b,c], Mamat Sawut [a,b,c], Mario Caetano [e]

[a] Center for Sustainability, Saint Louis University, Saint Louis, MO 63103, USA
[b] College of Resources and Environmental Sciences, Xinjiang University, Urumqi, Xinjiang 830046, China
[c] Ministry of Education Key Laboratory of Oasis Ecology at Xinjiang University, Urumqi, Xinjiang 830046, China
[d] Institute of New Imaging Technologies, Universidad Jaume I, 12071 Castellón, Spain
[e] Instituto Superior de Estatística e Gestão de Informação, Universidade Nova de Lisboa (ISEGI-NOVA), 1070-312 Lisboa, Portugal

ARTICLE INFO

Article history:
Received 27 September 2013
Received in revised form 20 December 2013
Accepted 28 December 2013

Keywords:
Land surface temperature
Landscape metrics
Normalized mutual information measure
Remote sensing
Sustainable urban planning
Urban heat island
Urban green space

ABSTRACT

The urban heat island (UHI) refers to the phenomenon of higher atmospheric and surface temperatures occurring in urban areas than in the surrounding rural areas. Mitigation of the UHI effects via the configuration of green spaces and sustainable design of urban environments has become an issue of increasing concern under changing climate. In this paper, the effects of the composition and configuration of green space on land surface temperatures (LST) were explored using landscape metrics including percentage of landscape (PLAND), edge density (ED) and patch density (PD). An oasis city of Aksu in Northwestern China was used as a case study. The metrics were calculated by moving window method based on a green space map derived from Landsat Thematic Mapper (TM) imagery, and LST data were retrieved from Landsat TM thermal band. A normalized mutual information measure was employed to investigate the relationship between LST and the spatial pattern of green space. The results showed that while the PLAND is the most important variable that elicits LST dynamics, spatial configuration of green space also has significant effect on LST. Though, the highest normalized mutual information measure was with the PLAND (0.71), it was found that the ED and PD combination is the most deterministic factors of LST than the unique effects of a single variable or the joint effects of PLAND and PD or PLAND and ED. Normalized mutual information measure estimations between LST and PLAND and ED, PLAND and PD and ED and PD were 0.7679, 0.7650 and 0.7832, respectively. A combination of the three factors PLAND, PD and ED explained much of the variance of LST with a normalized mutual information measure of 0.8694. Results from this study can expand our understanding of the relationship between LST and street trees and vegetation, and provide insights for sustainable urban planning and management under changing climate.

1. Introduction

The urban heat island (UHI) refers to the phenomenon of higher atmospheric and surface temperatures occurring in urban areas than in the surrounding rural areas. This phenomenon is widely observed in cities regardless of their sizes and locations (Connors et al., 2013; Cui and de Foy, 2012; Imhoff et al., 2010; Li et al., 2012; Tran et al., 2006). The UHI is mainly caused by the modification of land surfaces by urban development, which uses materials that effectively store short-wave radiation (Solecki et al., 2005). As a result, land surface temperature (LST) increases due to the UHI, which may disrupt species composition and distribution (Niemelä, 1999) by increasing the length of growing seasons, decrease air quality (Feizizadeh and Blaschke, 2013; Lai and Cheng, 2009; Sarrat et al., 2006; Weng and Yang, 2006), leading to greater health risks (Patz et al., 2005). The UHI may also decrease water quality as warmer waters flow into streams putting additional stress on aquatic ecosystems (James, 2002). Therefore, it has become a major research focus in urban climatology and urban ecology since first reported in 1818 (Howard, 1818).

The intensity and spatial pattern of UHI are largely exacerbated from population dynamics and development of build-up areas (Arnfield, 2003; Wu et al., 2013). Specifically, urban structure

* Corresponding author. Tel.: +1 314 977 7062
E-mail address: awulamu@slu.edu (A. Ghulam).

0924-2716/$ - see front matter
http://dx.doi.org/10.1016/j.isprsjprs.2013.12.010

(e.g., height-to-width ratio of buildings and streets), proportion of built-up versus green spaces per unit area, weather conditions (e.g., wind and humidity), and socioeconomic activities determine the development of the UHI (Hamdi and Schayes, 2007; Rizwan et al., 2008b; Taha, 1997; Unger, 2004; Voogt and Oke, 1998). For example, Huang et al. (2011) found statistically significant relationship between the UHI and socioeconomic factors indicating that higher UHI effects were linked to block groups characterized by low income, high poverty, less education, more ethnic minorities, more elderly people and greater risk of crime. As many of these factors, especially land surface characteristics are primarily represented by land-cover and land-use (LCLU), the relationship between the LST and LCLU has been the focus of numerous studies on the UHI (Buyantuyev and Wu, 2010; Dousset and Gourmelon, 2003; Pu et al., 2006; Voogt and Oke, 2003;Weng et al., 2004). This is due to the fact that vegetation usually has higher evapotranspiration and lower emissivity than built-up areas, and thus has lower surface temperatures (Hamada and Ohta, 2010; Weng et al., 2004).

Composition and configuration of green spaces are the two major elements of LCLU. The former refers to the abundance and variety of land cover types and the latter is related to the spatial arrangements and layout of land cover types (Connors et al., 2013; Turner, 2005). Remarkable proliferations of studies focusing on the relationship between LST and green space composition has been reported over the last two decades (Chen et al., 2006; Tran et al., 2006; Voogt and Oke, 2003; Weng, 2009; Weng et al., 2004). Though the magnitude of correlations varied among these reports, a negative relationship between the vegetation amount/fraction and LST was consistently observed. However, the spatial characteristics and configurations of vegetation patches within the urban environment have significant impacts on the distribution of the UHI (Bowler et al., 2010; Cao et al., 2010; Honjo and Takakura, 1991; Yokohari et al., 1997; Zhao et al., 2011), and that the size and shape of a vegetation patch creates cool island effects, a phenomenon that the temperature of green space is lower than its surrounding areas (Cao et al., 2010; Zhang et al., 2009). Based on a case study of a heavily urbanized Beijing metropolitan area in China, Li et al. (2012) also indicated that increasing patch density results in significantly higher LST when the size of urban green space unaffected, and that spatial configuration has a significant influence in the variability of derived LST.

It is evident from an exhaustive literature review hitherto that there is a lack of case studies within arid regions (Connors et al., 2013). As cities are growing fast in population, and urbanization is projected to be high (Baker et al., 2004), sustainable planning of urban environment to mitigate UHI effects highlights a pressing need for immediate attention. This is further emphasized by climate changes as arid regions are likely to become even drier in response to increasing temperature from global warming (Durack et al., 2012). Driven by fast economic growth and population increase, Northwestern China has experienced rapid urbanization in the past several decades, along with a drastic transformation of the urban environment and social equity (Aishan et al., 2013; Fan and Qi, 2010; Halik et al., 2013; Liu et al., 2013). In addition, the majority of the previous studies used ordinary least squares regression and/or spatial autoregression to analyze the relationship between the landscape metrics and LST. The statistical significance of the relationship between the landscape metrics and LST varied between the methods (Li et al., 2012). Comparative approaches with additional case studies are needed to generalize the methods and concepts demonstrated by these preliminary attempts. To that end, we investigate the effects of composition and configuration of urban green space on LST using a robust moving window algorithm of normalized mutual information measure in the arid city of Aksu, Xinjiang Uyghur Autonomous Region in Northwestern China. One of the advantages of using mutual information measures is that it can capture linear as well as strongly non-linear relationships among variables under the "umbrella" of just one concept ("mutual information"). The goal is to provide guiding suggestions for sustainable urban planning and development under future climate changes. We chose to use Landsat 30 m resolution data as previous studies (Liu and Weng, 2008; Li et al., 2013) have demonstrated that 30 m and 90 m are the optimal resolutions to study the relationship between LST and landscape patterns at patch level and landscape levels, respectively.

The paper is organized in the sections below. Following the description of the study area in Section 2, the methodology of calculating LST, landscape metrics, and a brief introduction to normalized mutual information measure are presented in Section 3. The results, discussions and conclusions are presented in Sections 4–6, respectively.

2. Study area

The study area, downtown Aksu City, Northwestern China, is a typical oasis city located in an arid region. Aksu City is the capital of Aksu Prefecture in Xinjiang Uyghur Autonomous Region, China. Geographically, the city is situated in south of the Tianshan Mountains and northwest edge of the Tarim Basin (39°30′N–41°27′N, 79°39′E–82°01′E; Fig. 1). Aksu City is known as "the Land of Melons and Fruits". It includes municipal total area of 14,300 km^2 and built-up area of 28.1 km^2.

Aksu City is rich in light and heat resources. It has a long frost-free period from 205 to 219 days. The climate is dry, and rainfall is extremely rare with less than 50 mm per year and average annual evaporation of 1950 mm. Topography of the study area is flat. The climatic and the physiographic conditions are mostly the same across the region. Therefore, it is an ideal area to explore the relationship between LST and spatial pattern of green space in arid and semi-arid land.

The proportion of green area in the metropolitan region has increased to 30.6% today from 12% in early 1980s. Urban green space coverage has reached 39.2% with the per capita public green area of 9 m^2. Meanwhile, city's ecological environment has been significantly improved. This rapid growth in green space emphasizes a need to develop most effective configuration of green space to reduce the urban heat island caused by expanding impervious surfaces and to adapt to the global climate change.

3. Methodology

3.1. Land surface temperature

Landsat-5 Thematic Mapper (TM) thermal infrared band 6 (11.45–12.50 μm) data with 120 × 120 m resolution were utilized to derive the LST (Fig. 2b). The satellite data were collected on August 19, 2011, which was a clear day with 0% cloud cover. Meteorological variables that influence the intensity of urban heat environment at the time of image capture were obtained from China standard meteorological station in the study site. These variables include daily precipitation (0 mm), daily average wind speed (1.6 m/s), wind direction (South-East) and humidity (46%). Due to the lack of detailed in situ atmospheric variables that allow physical inversion of brightness temperature to LST, a mono-window algorithm was applied for retrieval of LST (Qin et al., 2001)

$$T_S = [a(1 - C - D) + (b(1 - C - D) + C + D)T_{sensor} - DT_a]/C \quad (1)$$

with $C = \varepsilon\tau$, $D = (1 - \tau)$ $[1 + (1 - \varepsilon)$ $\tau]$, $\alpha = -67.355351$ and $b = 0.458606$, where ε land surface emissivity (LSE) is, τ is the total atmospheric transmissivity, T_{sensor} is the at-sensor brightness temperature, and T_a represents the mean atmospheric temperature given by:

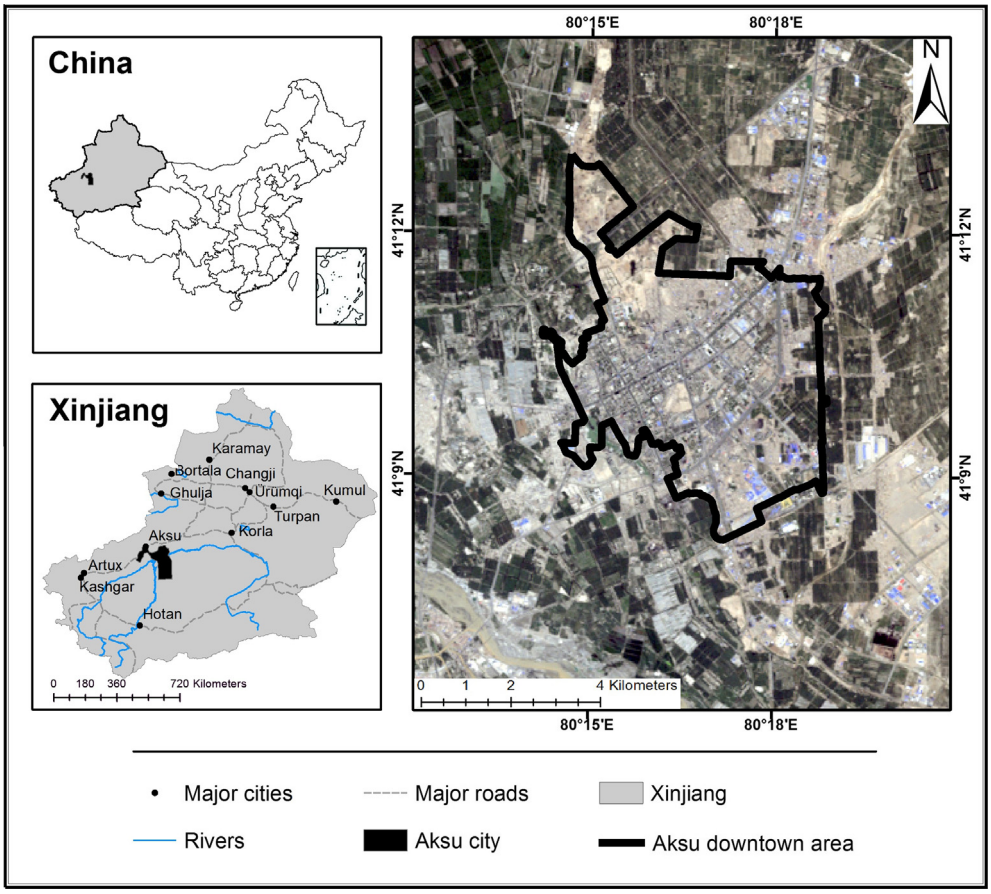

Fig. 1. Location map of the study area showing overview map of China (top – left corner) and the Xinjiang Uyghur Autonomous Region (bottom – left corner).

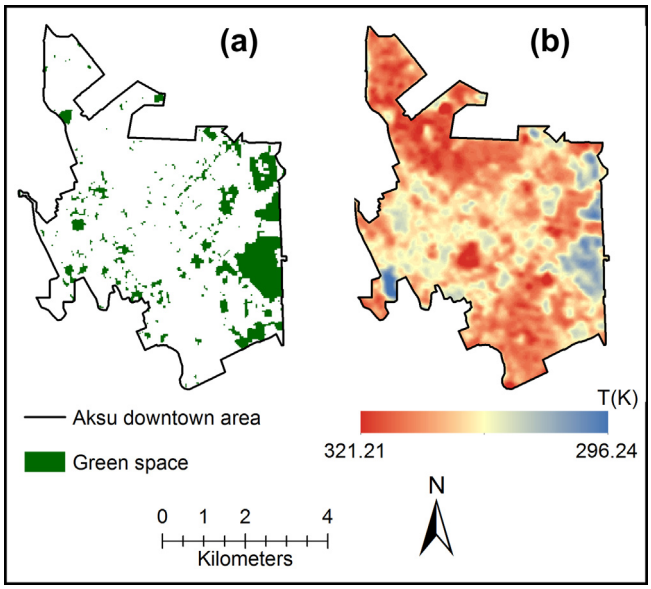

Fig. 2. Green space and LST maps for the downtown are Aksu city: (a) green space map and (b) LST map with units of Kelvin.

$$T_a = 16.011 + 0.92621T_0 \tag{2}$$

with T_0 being the near-surface air temperature. Qin et al. (2001) also estimated the atmospheric transmissivity from w, the atmospheric water vapor content, for the range 0.4–1.6 g/cm^2, according to the following equations:

$$\tau = 0.97429 - 0.08007w, \text{ and} \tag{3}$$

$$\tau = 0.982007 - 0.09611w \tag{4}$$

Both T_0 and w were obtained from local meteorological stations. LSE was obtained from the NDVI thresholds method (Sobrino et al., 2004).

$$\varepsilon = \varepsilon_{soil}, \text{ when NDVI} < 0.2, \tag{5}$$

$$\varepsilon = \varepsilon_{veg}, \text{ when NDVI} > 0.5 \text{ and} \tag{6}$$

$$\varepsilon = \varepsilon_{veg}P_v + d\varepsilon, \text{ when } 0.2 \geqslant \text{NDVI} \leqslant 0.5, \tag{7}$$

where ε_{soil} is the soil emissivity, ε_{veg} is the vegetation emissivity, and $d\varepsilon$ includes the effects of the geometry of natural surfaces and the internal reflections. Because most of the study area is a plain surface, this term is negligible. P_v is the fraction of the vegetation that can be computed by the following formula (Carlson and Ripley, 1997):

$$P_v = \left[\frac{NDVI - NDVI_{\min}}{(NDVI_{\max} - NDVI_{\min})}\right]^2 \tag{8}$$

where $NDVI_{\max} = 0.5$, and $NDVI_{\min} = 0.2$. Soil and vegetation emissivities were estimated to be 0.97 and 0.99, respectively (Sobrino et al., 2004).

3.2. Spatial pattern of green space

The multi-spectral Landsat-5 TM data acquired on August 19, 2011 were used to map green space (i.e., vegetated areas) (Fig. 2a). The spatial resolution of the multi-spectral data is 30 m.

A maximum likelihood image classification approach was applied to extract the vegetated area using ENVI from EXELIS Visual Information Solutions. The four bands green, red, near-infrared, and two shortwave infrared were used for classification. An accuracy assessment was conducted based on 200 ground reference data that were photo interpreted from existing land cover map with a scale of 1:150000 (produced by Land Resources Bureau of Aksu City and College of Resources and Environmental Sciences, Xinjiang University, China in June, 2012) together with Landsat true color image. The overall accuracy of the derived classification map was 87.60%, and the kappa coefficient was 0.83 (Table 1).

It has been demonstrated that land surface temperature or surface urban heat island could be related to LCLU types (Chen et al., 2006; Connors et al., 2013; Weng, 2001; Xian and Crane, 2006), and there are relationships between spatial structure of urban thermal patterns and urban surface characteristics (Li et al., 2011; Liu and Weng, 2008; Weng et al., 2007). The last several decades have witnessed a remarkable proliferation of studies on developing landscape metrics (1) to characterize landscape patterns and its association to UHIs (Gustafson, 1998; Li and Reynolds, 1993; Li and Wu, 2004; McGarigal and Marks, 1995; Turner, 2005; Turner et al., 1989; Wu, 2000; Wu et al., 2002), and (2) to relate landscape patterns to ecological processes (Turner, 2005). With respect to the measurement objectives, these metrics can be generalized into landscape composition and spatial configuration metrics (Gustafson, 1998; McGarigal and Marks, 1995). Landscape composition metrics measure the presence and amount of different patch types within the landscape without explicitly describing its spatial features while landscape configuration metrics measure the spatial distribution of patches within the landscape (Alberti, 2005). In this study, we selected three commonly occurring landscape metrics to relate LST with spatial pattern of urban green space according to the following principles (Lee et al., 2009; Li and Wu, 2004; Riitters et al., 1995; Riva-Murray et al., 2010): (1) important in both theory and practice, (2) easily calculated, (3) interpretable, and (4) minimal redundancy. Table 2 shows the three landscape metrics. See Mcgarigal et al. (2002) for detailed calculation equation and comments. They are selected to provide complementary information about landscape structure for both composition and configuration.

The metrics were calculated using the landscape structure analysis program FRAGSTATS (http://www.umass.edu/landeco/research/fragstats/fragstats.html). The FRAGSTATS software allows the option of conducting a local structure gradient or moving window analysis, and generating the results as a new grid for each selected metric. Our choice was to use moving window analysis, which requires a user specifies the level of heterogeneity (class or landscape) and the shape (round, square or hexagon) and size (radius or length of side, in meters) of the window to be used. A window of the specified shape and size is passed over all positively valued cells inside the landscape of interest. However, only cells in which the entire window is contained within the landscape are evaluated. Within each window, the selected metric at the class or landscape level is computed, and the value is returned to the focal cell. The moving window is passed over the grid until every positively valued cell containing a full window is assessed in this manner.

Table 2
Landscape metrics used in this study (Mcgarigal et al., 2002).

Metrics (abbreviation)	Calculation and description
Compositional	$100/A \times \sum_{i=1}^{n} a_i$
Percentage of landscape (PLAND)	Proportional abundance of green space in the landscape (%)
Configurational	$n/A \times 10^6$
Patch density (PD)	Number of green space patches divided by total landscape area (n/km^2)
Edge density (ED)	$10,000/A \times \sum_{i=1}^{n} e_i$ Total length (border not included) of all edge segments of green space per hectare (m/ha)

a_i, area of patch i; e_i, length of edge (or perimeter) of patch i; A, landscape area; n, number of patches.

In our case, we used 8-cell rule which considers all eight adjacent cells that share a side with the focal cell and 500 m-radius circular window. The window moves over the landscape one cell at a time, calculating the selected metric within the window and returning that value to the center cell and output a new continuous surface grid map for each selected metric (Mcgarigal et al., 2002).

3.3. Statistical correlation measures

Scatter plots were generated to explore the bivariate relationship between LST and each of the landscape metrics. The normalized mutual information measure was assessed based on them (Cover and Thomas, 1991; Webb, 2002). The Shannon entropy of a continuous random variable X with probability density function $p(x)$ for all possible events $x \in S$ is defined as

$$H(X) = -\int_S p(x) \log p(x) dx \tag{9}$$

where S is the support of the variable and $p(x)$ is its probability distribution function. Probability distributions may be used to construct a frequency distribution of certain events occurring either discretely, in the form of a histogram, or continuously (Allaby, 2008).

In the case of a discrete random variable X, entropy $H(X)$ is expressed as

$$H(X) = -\sum_{x \in \Omega} p(x) \log p(x) \tag{10}$$

where $p(x)$ represents the probability of an event $x \in \Omega$ from a finite set (Ω) of possible values.

In probability and information theories, the mutual information of two random variables is a quantity that measures the amount of

Table 1
Accuracy assessment of the urban green space classification map.

	Reference data (pixels)					User's accuracy (%)
	Urban green space	Residential area	Construction site	Water body	Total	
Urban green space	231	6	2	2	241	95.9
Residential area	0	170	15	2	187	90.9
Construction site	1	53	148	2	202	73.3
Water body	0	11	0	99	110	90.0
Total	232	240	165	103	740	
Producer's accuracy (%)	99.6	70.8	89.7	96.1		
Overall accuracy (%)	87.6					
Kappa coefficient	0.83					

information that both variables share. Formally, the mutual information of two discrete random variables X and Y can be defined as:

$$I(X,Y) = \sum_{x\in X}\sum_{y\in Y} p(x,y)\log\left(\frac{p(x,y)}{p(x)p(y)}\right) \quad (11)$$

where $p(x,y)$ is the joint probability function of X and Y, defined as

$$p(x,y) = P(X = x \text{ and } Y = y) \quad (12)$$

We can define:

$$p(x) = \sum_{y\in A} p(X = x, y) \quad (13)$$

$$p(y) = \sum_{x\in A} p(x, Y = y) \quad (14)$$

as the marginal probability distribution functions of X and Y respectively.

$I(x,y)$ is always a non-negative quantity, being zero when the variables are statistically independent. The higher the value of I, the higher is the dependence between them.

The normalized mutual information (Cover and Thomas, 1991; Sridhar et al., 1998), can be defined as

$$C_{XY} = \frac{I(X;Y)}{H(Y)} \text{ and } C_{YX} = \frac{I(X;Y)}{H(X)} \quad (15)$$

This expression can be used as a "correlation" measure (Cover and Thomas, 1991) with the advantage of capturing linear and non-linear relationships among variables. It is sometimes called as "asymmetric dependency coefficient (ADC)" (Sridhar et al., 1998). However, two definitions in Eq. (15) will produce unequal values due to their asymmetric property in the definitions. Therefore, a symmetric normalized mutual information measure can be proposed (Press et al., 1990; Strehl and Ghosh, 2003), such as

$$NI(X,Y) = 2\frac{I(X,Y)}{H(Y)+H(X)}, \quad NI(X,Y) = \frac{I(X,Y)}{\sqrt{H(Y)H(X)}} \quad (16)$$

It is worth mentioning that the mutual information of two random variables $I(X,Y)$ is always smaller than the entropy of any of them, i.e., $H(X)$ or $H(Y)$, namely: $I(X;Y) < H(Y)$ and $I(X;Y) < H(X)$ are valid, because the information both variables share can never be greater than the information each one has. Therefore $0 \leqslant C_{XY} \leqslant 1$. If C_{XY} equals one, it means X, Y are perfectly correlated. If C_{XY} equals 0 it indicates there is no correlation between X, Y.

In this study, Eq. (15)was applied to measure the normalized mutual information between the different variables since the focus of the work is to find out the correlation between the land surface temperature, which is chosen as a proxy of target variable, and other variables including PLAND, PD and ED.

4. Results

The spatial distribution of PLAND is shown in (Fig. 3a), PD (Fig. 3b) and ED (Fig. 3c). Higher vegetation cover or percent green space is located on the eastern edge of the study site, which is possibly a park or a nursery with mature grown trees (Fig. 3a). Patch density is high over the Middle-Western Aksu downtown (Fig. 3b) indicating more fragmented but evenly distributed vegetation patches. Edge density, an indicator of linear configuration of green space along the streets, appears to be large on southwest and northeast parts of the study site. The spatial distribution patterns of patch density and edge density are similar suggesting there exists some degree of correlation between these two variables.

Two dimensional scatter plots between LST and landscape metrics are shown in Fig. 4. There seems to be a negative linear relationship between LST and both vegetation fraction and edge density. However, these relationships do not seem to be statistically significant enough $R^2 < 0.32$ (in all cases) to obtain meaningful conclusions. That is why other measures may play an important role. However, some useful information can be extracted. It is interesting to note that patch density and edge density are correlated variables but demonstrates very different degrees of effects on LST. The results imply that edge density has more deterministic effects on LST than the patch density. One may expect that plantation of street trees evenly distributed in the urban area may be an effective way of reducing urban heat island effects, therefore, energy consumption as opposed to establishing dense patches of green space in discrete locations.

Table 3 shows the normalized mutual information analysis between the LST and landscape metrics calculated using Eq. (15). It is

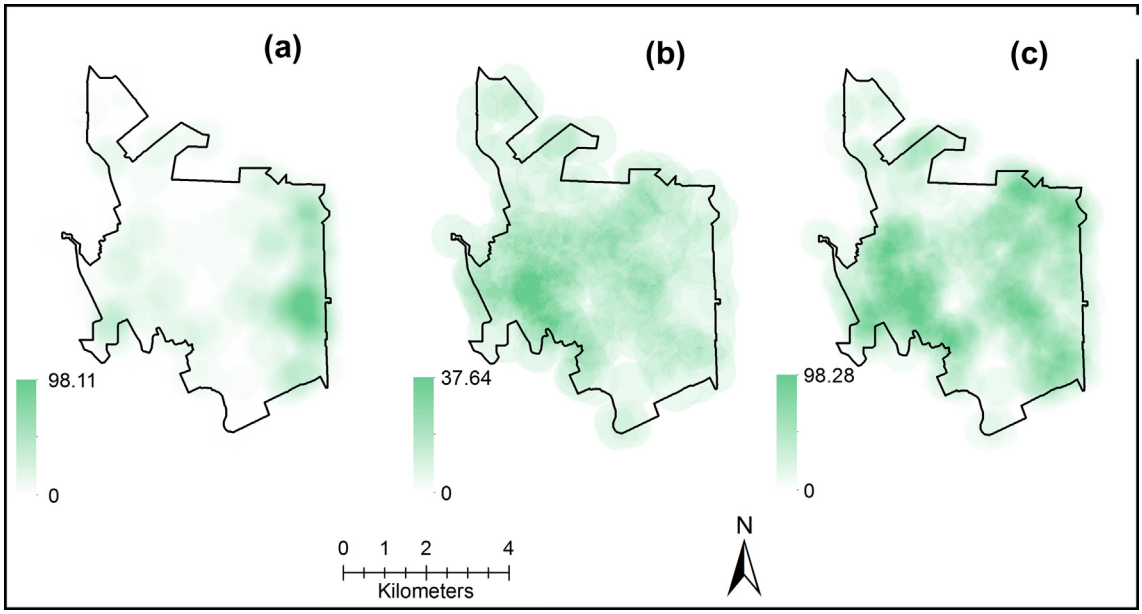

Fig. 3. Grid map of urban green space metrics. (a) Percent cover of green space, (b) patch density and (c) edge density.

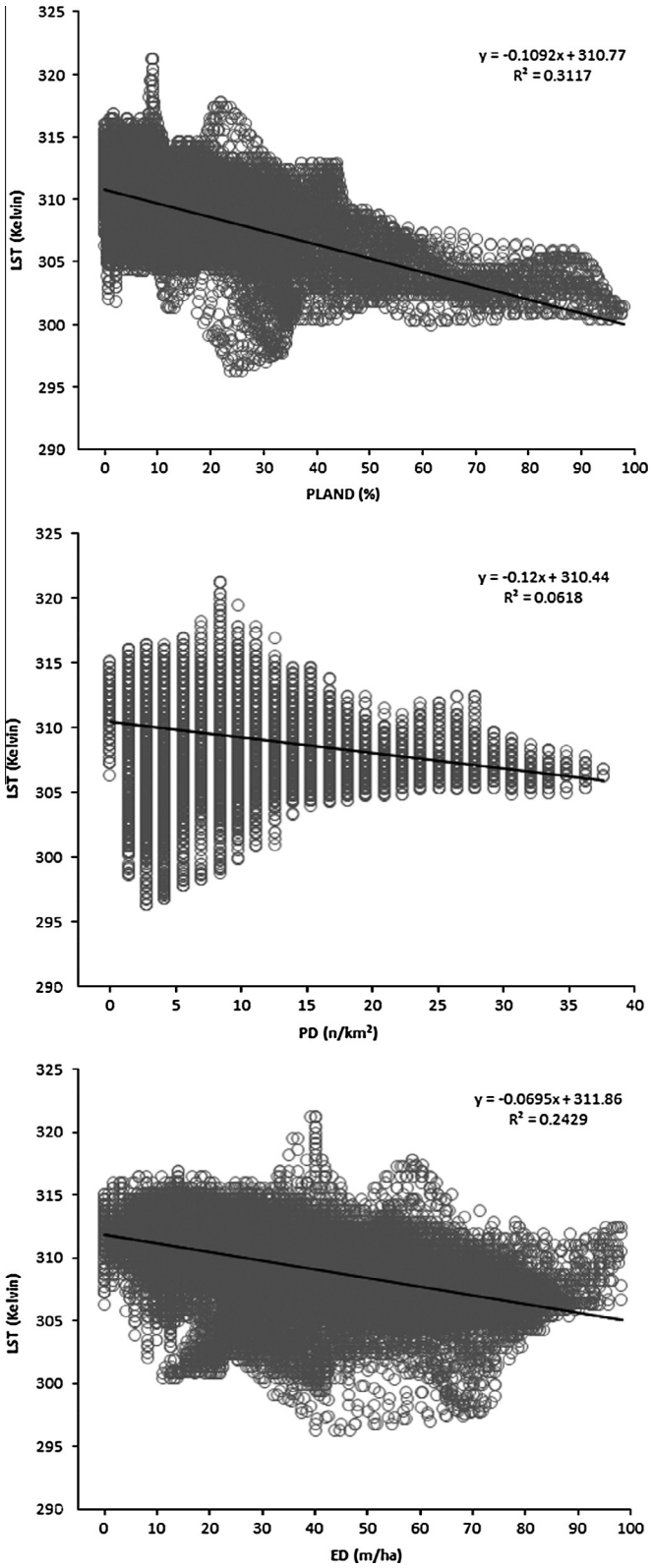

Fig. 4. Scatter plot of LST with PLAND, PD and ED.

evident that the compositional and spatial configuration of urban green space can affect the LST to a certain degree. When these two major categories of green space pattern are taken into account separately, it seems the compositional green space pattern has slightly larger effect on LST than configurational factors.

Table 3
Normalized mutual information results of compositional configuration of green space and landscape metrics.

C_{XY}		Normalized mutual information value
X	*Y*	
PLAND		0.7100
PD		0.6985
ED		0.7033
PLAND, PD	LST	0.7679
PLAND, ED		0.7650
PD, ED		0.7832
PLAND, PD, ED		0.8694

Meanwhile, the configurational green space patterns do have relatively strong effect but not as strong as compositional green space pattern. The mutual information value was largest when all three landscape metrics were considered in order to see the effect on the LST. This is expected since each of the landscape metrics does have some level of causal interactions with LST change, and the effects could constructively interfere each other. Combination of any two or three of the landscape metrics had a higher impact on LST than that of a single variable. The joint effect of (*PLAND*, *PD*) was slightly better in magnitude than the effect of (*PLAND*, *ED*) on LST, confirming the stronger correlation between edge density and LST as shown in Fig. 4. However, the mutual information value between (*ED*, *PD*) and LST was larger than of the (*PLAND*, *PD*) and (*PLAND*, *ED*), which might be attributed to the fact that (1) patch density and edge density is more determinative factors that elicits LST and (2) there exist correlations between patch density and edge density.

5. Discussion

The results of this study showed that PLAND was correlated with LST with statistical significance. This is consistent with a number of previous studies, which demonstrated negative correlations between LST and the abundance of green space measured by Normalized Difference Vegetation Index (Buyantuyev and Wu, 2010; Chen et al., 2006), fraction of vegetation (Weng et al., 2004), percent cover of LCLU (e.g., Forest, Grass, Cropland, etc.) (Weng et al., 2006; Zhou et al., 2011), or PLAND (Li et al., 2012). Trees and other plants help cool the environment, making green space a simple and effective way to mitigate urban heat island effects. Green spaces lower surface and air temperatures by evapotranspiration due to its lower thermal inertia compared to impervious surfaces and bare soils (Hamada and Ohta, 2010; Lambin and Ehrlich, 1996; Weng et al., 2004); by providing shade that prevents land surfaces from direct heating from sunlight (Zhou et al., 2011). Concerning the configurational metrics, the PD and ED were less correlated with LST than PLAND. The normalized mutual information analysis also showed that there was less dependence between the LST with individual PD and ED, which is still smaller than the dependence between the PLAND and LST. This indicates that the increase of patch density leads to a decrease in mean patch size resulting in a general increase in total patch edges. Therefore, the effects of the increase in patch density on LST can be explained by both a decrease in mean patch size and increase in patch edges. The decrease in mean patch size may increase LST because a larger, continuous green space produces stronger cool island effects than that of several small pieces of green space even if the total area equals to the area of the continuous green space (Cao et al., 2010; Li et al., 2012; Zhang et al., 2009). In contrast, the increase of total patch edges may enhance energy flow and exchange between green space and its surrounding areas, and provide more shade for surrounding surfaces, which lead to the decrease of LST (Zhou et al., 2011).

As far as the each landscape metric is concerned individually, the highest normalized mutual information measure was found with the PLAND (0.71). The implication from this observation is that the composition of green space was more important than the configuration of green space in reducing UHI effects, which is consistent with previous findings (Li et al., 2012; Zhou et al., 2011). However, our results also showed that ED and PD together were the most deterministic factors of LST than the unique effects of a single variable or the joint effects PLAND and PD or PLAND and ED. Normalized mutual information measure between LST and PLAND and ED, PLAND and PD and ED and PD were 0.7679, 0.7650 and 0.7832, respectively. A combination of the three factors PLAND, PD and ED explained much of the variance of LST with a normalized mutual information measure of 0.8694. This is because the composition and configuration of green space are constructively interrelated.

Many of the results from this study regarding to the relationships between the green space and LST were expected as reported in a number of publications (Connors et al., 2013; Hamada and Ohta, 2010; Li et al., 2011; Weng et al., 2004). Traditionally, increasing the green space by planting more trees has been emphasized in urban planning (Rizwan et al., 2008a; Zhou et al., 2011). While confirming the fact that the increase in green space can significantly mitigate UHI effects, our results showed that configuration of green space as expressed by the joint effect of PD and ED is the most deterministic metric that affects LST. Optimizing the configuration of green space which increases the PD and ED should be highlighted to mitigate UHI effects. These results have important implications for green space management, particularly in rapidly urbanizing arid regions as in our case study, where both water resources and available land area for increased green space is extremely limited.

Under changing climate, arid regions are likely to become even drier, while wet areas tend to get wetter in response to observed global warming (Durack et al., 2012) as indicated by increasing surface temperature. Expanding the urban green space is a rational approach for adapting to climate change. At the same time, it can contribute to the sustainable development of urban areas. However, it may compete with other socio-economic interests that also require space. Therefore, in order to determine a proper balance between the sustainable development and urban green space increase, urban planners should work on optimizing the configuration of green space patches in selected areas by increasing the size of existing green space patches rather than building new smaller patches. In the arid Northwestern China, where temperatures are already high and water resources are limited, the outcome of this study can support decisions about sustainable urban design and development, which will help mitigating the effects of future climate, and benefit human wellbeing by improving water and energy use efficiency.

6. Conclusion

Taking the urban area of the oasis city of Aksu area as an example, this study quantitatively examined the effects of spatial composition and configuration of green space on land surface temperature (LST). Normalized mutual information measure was used to quantify the relationship between LST and landscape metrics including percentage of landscape (PLAND), edge density (ED) and patch density (PD). Our results showed that (1) both the composition and configuration of green space elicits urban heat island; (2) joint effects of any two combinations of the metrics was larger than the effect of a single metric; (3) ED and PD combined was the most deterministic factor of LST than the unique effects of a single variable or the joint effects PLAND and PD or PLAND and ED; (4) optimizing the configuration of green space which increases the PD and ED should be prioritized in sustainable urban planning and development to mitigate urban heat island effects.

Water scarcity is the major limiting factor of anthropogenic activities in arid and semi-arid regions. Specifically, the increase of green space cover is restricted by water availability. Our results suggested that by increasing patch and edge density of the green space, the thermal environment in the City of Aksu can be further improved without expanding the percentage of landscape (PLAND). In arid and semi-arid regions, where temperatures are already high and water resources are limited, the outcome of this study may provide climate change adaptation and mitigation benefits by reducing greenhouse gas emissions and energy demand for the cooling of buildings.

Acknowledgments

The first author would like to express his gratitude to the European Commission and Erasmus Mundus Consortium for their important scholarship for master students. We acknowledge the National Natural Science Foundation of China (#s: 31270742, U1138303, 41130531, 41361016), Sino-German joint research project SuMaRiO (01LL0918C), Research Foundation of Xinjiang University (BS120116 and XY110117) and Education Department of Xinjiang Uyghur Autonomous Region (XJEDU2011S07) for financially supporting this work. Finally, we also extend our gratitude to the anonymous reviewers of this manuscript for their helpful suggestions.

References

Aishan, T., Halik, Ü., Cyffka, B., Kuba, M., Abliz, A., Baidourela, A., 2013. Monitoring the hydrological and ecological response to water diversion in the lower reaches of the Tarim River. Northwest China. Quatern. Int. 311, 155–162.
Alberti, M., 2005. The effects of urban patterns on ecosystem function. Int. Regional Sci. Rev. 28, 168–192.
Allaby, M., 2008. A Dictionary of Earth Sciences, third ed. Oxford University Press Inc., New York, pp. 460.
Arnfield, A.J., 2003. Two decades of urban climate research: a review of turbulence, exchanges of energy and water, and the urban heat island. Int. J. Climatol. 23, 1–26.
Baker, L.A., Brazel, A.J., Westerhoff, P., 2004. Environmental consequences of rapid urbanization in warm, arid lands: case study of Phoenix, Arizona (USA). In: Marchettini, N., Brebbia, C., Tiezzi, E., Wadhwa, L.C. (Eds.), The Sustainable City III, (Proceedings of the Sienna Conference, held June 2004), Advances in Architecture Series. WIT Press, Boston.
Bowler, D.E., Buyung-Ali, L., Knight, T.M., Pullin, A.S., 2010. Urban greening to cool towns and cities: a systematic review of the empirical evidence. Landscape Urban Plan. 97, 147–155.
Buyantuyev, A., Wu, J., 2010. Urban heat islands and landscape heterogeneity: linking spatiotemporal variations in surface temperatures to land-cover and socioeconomic patterns. Landscape Ecol. 25, 17–33.
Cao, X., Onishi, A., Chen, J., Imura, H., 2010. Quantifying the cool island intensity of urban parks using ASTER and IKONOS data. Landscape Urban Plan. 96, 224–231.
Carlson, T.N., Ripley, D.A., 1997. On the relation between NDVI, fractional vegetation cover, and leaf area index. Remote Sens. Environ. 62, 241–252.
Chen, X.L., Zhao, H.M., Li, P.X., Yin, Z.Y., 2006. Remote sensing image-based analysis of the relationship between urban heat island and land use/cover changes. Remote Sens. Environ. 104, 133–146.
Connors, J.P., Galletti, C.S., Chow, W.T.L., 2013. Landscape configuration and urban heat island effects: assessing the relationship between landscape characteristics and land surface temperature in Phoenix, Arizona. Landscape Ecol. 28, 271–283.
Cover, T., Thomas, J., 1991. Elements of Information Theory. Wiley-Interscience.
Cui, Y.Y., de Foy, B., 2012. Seasonal variations of the urban heat island at the surface and the near-surface and reductions due to urban vegetation in Mexico City. J. Appl. Meteorol. Climatol. 51, 855–868.
Dousset, B., Gourmelon, F., 2003. Satellite multi-sensor data analysis of urban surface temperatures and landcover. ISPRS J. Photogramm. Remote Sens. 58, 43–54.
Durack, P.J., Wijffels, S.E., Matear, R.J., 2012. Ocean salinities reveal strong global water cycle intensification during 1950 to 2000. Science 336, 455–458.
Fan, P., Qi, J., 2010. Assessing the sustainability of major cities in China. Sustain. Sci. 5, 51–68.
Feizizadeh, B., Blaschke, T., 2013. Examining urban heat island relations to land use and air pollution: multiple endmember spectral mixture analysis for thermal remote sensing. IEEE J. Sel. Top. Appl. Earth Obs. Remote Sens. 6, 1749–1756.

Gustafson, E.J., 1998. Quantifying landscape spatial pattern: what is the state of the art? Ecosystems 1, 143–156.
Halik, W., Mamat, A., Dang, J.H., Deng, B.S.H., Tiyip, T., 2013. Suitability analysis of human settlement environment within the Tarim Basin in Northwestern China. Quatern. Int. 311, 175–180.
Hamada, S., Ohta, T., 2010. Seasonal variations in the cooling effect of urban green areas on surrounding urban areas. Urban Forest. Urban Greening 9, 15–24.
Hamdi, R., Schayes, G., 2007. Sensitivity study of the urban heat island intensity to urban characteristics. Int. J. Climatol. 28, 973–982.
Honjo, T., Takakura, T., 1991. Simulation of thermal effects of urban green areas on their surrounding areas. Energy Build. 15, 443–446.
Howard, L., 1818. The Climate of London, Deduced from Meteorological Observations, Made at Different Places in the Neighbourhood of the Metropolis, vol. 2, W. Phillips, London, pp. 1818–1820.
Huang, G., Zhou, W., Cadenasso, M.L., 2011. Is everyone hot in the city? Spatial pattern of land surface temperatures, land cover and neighborhood socioeconomic characteristics in Baltimore, MD. J. Environ. Manage. 92, 1753–1759.
Imhoff, M.L., Zhang, P., Wolfe, R.E., Bounoua, L., 2010. Remote sensing of the urban heat island effect across biomes in the continental USA. Remote Sens. Environ. 114, 504–513.
James, W., 2002. Green roads: research into permeable pavers. Stormwater 3, 48–50.
Lai, L.-W., Cheng, W.-L., 2009. Air quality influenced by urban heat island coupled with synoptic weather patterns. Sci. Total Environ. 407, 2724–2733.
Lambin, E., Ehrlich, D., 1996. The surface temperature–vegetation index space for land cover and land-cover change analysis. Int. J. Remote Sens. 17, 463–487.
Lee, S.-W., Hwang, S.-J., Lee, S.-B., Hwang, H.-S., Sung, H.-C., 2009. Landscape ecological approach to the relationships of land use patterns in watersheds to water quality characteristics. Landscape Urban Plan. 92, 80–89.
Li, H., Reynolds, J.F., 1993. A new contagion index to quantify spatial patterns of landscapes. Landscape Ecol. 8, 155–162.
Li, H., Wu, J., 2004. Use and misuse of landscape indices. Landscape Ecol. 19, 389–399.
Li, J., Song, C., Cao, L., Zhu, F., Meng, X., Wu, J., 2011. Impacts of landscape structure on surface urban heat islands: a case study of Shanghai, China. Remote Sens. Environ. 115, 3249–3263.
Li, X., Zhou, W., Ouyang, Z., Xu, W., Zheng, H., 2012. Spatial pattern of greenspace affects land surface temperature: evidence from the heavily urbanized Beijing metropolitan area, China. Landscape Ecol. 27, 887–898.
Li, X., Zhou, W., Ouyang, Z., 2013. Relationship between land surface temperature and spatial pattern of greenspace: what are the effects of spatial resolution? Landscape Urban Plan. 114, 1–8.
Liu, H., Weng, Q., 2008. Seasonal variations in the relationship between landscape pattern and land surface temperature in Indianapolis, USA. Environ. Monit. Assess. 144, 199–219.
Liu, G., Kurban, A., Duan, H., Halik, Ü., Ablekim, A., Zhang, L., 2013. Desert riparian forest colonization in the lower reaches of Tarim River based on remote sensing analysis. Environ. Earth Sci. http://dx.doi.org/10.1007/s12665-013-2850-9.
McGarigal, K., Marks, B.J., 1995. Spatial Pattern Analysis Program for Quantifying Landscape Structure. Gen. Tech. Rep. PNW-GTR-351. US Department of Agriculture, Forest Service, Pacific Northwest Research Station.
Mcgarigal, K., Cushman, S., Neel, M., Ene, E., 2002. FRAGSTATS: Spatial Pattern Analysis Program for Categorical Maps.
Niemelä, J., 1999. Ecology and urban planning. Biodivers. Conserv. 8, 119–131.
Patz, J.A., Campbell-Lendrum, D., Holloway, T., Foley, J.A., 2005. Impact of regional climate change on human health. Nature 438, 310–317.
Press, W.H., Flannery, B.P., Teukolsky, S.A., Vetterling, W.T., 1990. Numerical Recipes. Cambridge Univ. Press.
Pu, R., Gong, P., Michishita, R., Sasagawa, T., 2006. Assessment of multi-resolution and multi-sensor data for urban surface temperature retrieval. Remote Sens. Environ. 104, 211–225.
Qin, Z.-H., Karnieli, A., Berliner, P., 2001. A mono-window algorithm for retrieving land surface temperature from Landsat TM data and its application to the Israel–Egypt border region. Int. J. Remote Sens. 22, 3719–3746.
Riitters, K.H., O'neill, R., Hunsaker, C., Wickham, J.D., Yankee, D., Timmins, S., Jones, K., Jackson, B., 1995. A factor analysis of landscape pattern and structure metrics. Landscape Ecol. 10, 23–39.
Riva-Murray, K., Riemann, R., Murdoch, P., Fischer, J.M., Brightbill, R., 2010. Landscape characteristics affecting streams in urbanizing regions of the Delaware River Basin (New Jersey, New York, and Pennsylvania, US). Landscape Ecol. 25, 1489–1503.
Rizwan, A.M., Dennis, L.Y., Liu, C., 2008a. A review on the generation, determination and mitigation of Urban Heat Island. J. Environ. Sci. 20, 120–128.
Rizwan, A.M., Dennis, L.Y.C., Liu, C., 2008b. A review on the generation, determination and mitigation of Urban Heat Island. J. Environ. Sci. 20, 120–128.
Sarrat, C., Lemonsu, A., Masson, V., Guedalia, D., 2006. Impact of urban heat island on regional atmospheric pollution. Atmos. Environ. 40, 1743–1758.
Sobrino, J.A., Jiménez-Muñoz, J.C., Paolini, L., 2004. Land surface temperature retrieval from LANDSAT TM 5. Remote Sens. Environ. 90, 434–440.
Solecki, W.D., Rosenzweig, C., Parshall, L., Pope, G., Clark, M., Cox, J., Wiencke, M., 2005. Mitigation of the heat island effect in urban New Jersey. Global Environ. Change B: Environ. Hazards 6, 39–49.
Sridhar, D.V., Bartlett, E.B., Seagrave, R.C., 1998. Information theoretic subset selection for neural network models. Comput. Chem. Eng. 22, 613–626.
Strehl, A., Ghosh, J., 2003. Cluster ensembles – a knowledge reuse framework for combining multiple partitions. J. Mach. Learn. Res. 3, 583–617.
Taha, H., 1997. Urban climates and heat islands: albedo, evapotranspiration, and anthropogenic heat. Energy Build. 25, 99–103.
Tran, H., Uchihama, D., Ochi, S., Yasuoka, Y., 2006. Assessment with satellite data of the urban heat island effects in Asian mega cities. Int. J. Appl. Earth Obs. Geoinf. 8, 34–48.
Turner, M.G., 2005. Landscape ecology: what is the state of the science? Annu. Rev. Ecol. Evol. Syst., 319–344.
Turner, M.G., O'Neill, R.V., Gardner, R.H., Milne, B.T., 1989. Effects of changing spatial scale on the analysis of landscape pattern. Landscape Ecol. 3, 153–162.
Unger, J., 2004. Intra-urban relationship between surface geometry and urban heat island: review and new approach. Clim. Res. 27, 253–264.
Voogt, J.A., Oke, T., 1998. Effects of urban surface geometry on remotely-sensed surface temperature. Int. J. Remote Sens. 19, 895–920.
Voogt, J.A., Oke, T.R., 2003. Thermal remote sensing of urban climates. Remote Sens. Environ. 86, 370–384.
Webb, A.R., 2002. Statistical Pattern Recognition. Wiley.
Weng, Q., 2001. A remote sensing? GIS evaluation of urban expansion and its impact on surface temperature in the Zhujiang Delta, China. Int. J. Remote Sens. 22, 1999–2014.
Weng, Q., 2009. Thermal infrared remote sensing for urban climate and environmental studies: methods, applications, and trends. ISPRS J. Photogramm. Remote Sens. 64, 335–344.
Weng, Q., Yang, S., 2006. Urban air pollution patterns, land use, and thermal landscape: an examination of the linkage using GIS. Environ. Monit. Assess. 117, 463–489.
Weng, Q., Lu, D., Schubring, J., 2004. Estimation of land surface temperature–vegetation abundance relationship for urban heat island studies. Remote Sens. Environ. 89, 467–483.
Weng, Q., Lu, D., Liang, B., 2006. Urban surface biophysical descriptors and land surface temperature variations. Photogramm. Eng. Remote Sens. 72, 1275–1286.
Weng, Q., Liu, H., Lu, D., 2007. Assessing the effects of land use and land cover patterns on thermal conditions using landscape metrics in city of Indianapolis, United States. Urban Ecosyst. 10, 203–219.
Wu, J., 2000. Landscape Ecology: Pattern, Process, Scale and Hierarchy, vol. 13. Higher Education Press, Beijing, pp. 121–123.
Wu, J., Shen, W., Sun, W., Tueller, P.T., 2002. Empirical patterns of the effects of changing scale on landscape metrics. Landscape Ecol. 17, 761–782.
Wu, C.-D., Lung, S.-C.C., Jan, J.-F., 2013. Development of a 3-D urbanization index using digital terrain models for surface urban heat island effects. ISPRS J. Photogramm. Remote Sens. 81, 1–11.
Xian, G., Crane, M., 2006. An analysis of urban thermal characteristics and associated land cover in Tampa Bay and Las Vegas using Landsat satellite data. Remote Sens. Environ. 104, 147–156.
Yokohari, M., Brown, R.D., Kato, Y., Moriyama, H., 1997. Effects of paddy fields on summertime air and surface temperatures in urban fringe areas of Tokyo, Japan. Landscape Urban Plan. 38, 1–11.
Zhang, X., Zhong, T., Feng, X., Wang, K., 2009. Estimation of the relationship between vegetation patches and urban land surface temperature with remote sensing. Int. J. Remote Sens. 30, 2105–2118.
Zhao, C., Fu, G., Liu, X., Fu, F., 2011. Urban planning indicators, morphology and climate indicators: a case study for a north–south transect of Beijing, China. Build. Environ. 46, 1174–1183.
Zhou, W., Huang, G., Cadenasso, M.L., 2011. Does spatial configuration matter? Understanding the effects of land cover pattern on land surface temperature in urban landscapes. Landscape Urban Plan. 102, 54–63.